Academic Misconduct Declaration

I ___________________________Natan Grayman_________ (student name and surname), ____________2344104_______ (student number), hereby declare that:

1. I have read the Student Academic Misconduct Policy [1] and I understand that "*Academic Misconduct includes any action which gains, attempts to gain, or assists others in gaining or attempting to gain an unfair academic benefit. It includes Plagiarism, collusion, cheating, copying, contract cheating, fabrication of data, the use and/or possession of unauthorised materials or devices during an assessment; and falsification or misrepresentation of information including, falsification of a medical certificate, and/or changing a script after it has been marked*" [1].
2. I know that any act of academic misconduct is unacceptable, and carries a penalty as prescribed in the Student Academic Misconduct Policy [1].
3. This assessment/submission for the course__________ELEN4006A____________is my own work and I have not engaged in any act of academic misconduct in the completion of this work.

Signature: ___________________________________ Date: _________8 May 2023___________

Reference:

[1] University of Witwatersrand, Student Academic Misconduct Policy G-C-2022-029, 2022.

Measurement Systems Project Part 2

Author: Natan Grayman

Student Number: 2344104

Date: 8 May 2023

Abstract: This report illustrates a light measurement system that is mounted onto a jungle gym designed for children in a park in Johannesburg, South Africa. Safety and visibility are paramount for children playing on a jungle gym; therefore, this design entails a measurement system that displays the given light intensity and switches on a light provided there is insufficient visible illumination. A pin-photodiode sensor has been chosen as specified in report 1. The required spectral input range, bandwidth of 5mHz and accuracy of 95% were achieved, ultimately providing a realistic and sustainable solution. This report presents the design specifications with a high-level solution, a detailed design of the system showing the logic of the micro-controller, a performance evaluation of all stages of the system and a critical analysis.

1. Introduction

This report illustrates a light measurement system that is mounted onto a jungle gym designed for children in a park in Johannesburg, South Africa. Safety and visibility are paramount for children playing on a jungle gym; therefore, this design entails a measurement system that displays the given light intensity and switches on a light provided there is insufficient visible illumination. A pin-photodiode sensor has been chosen as specified in report 1, which combined with signal conditioning and signal processing elements produces a reliable lighting measurement system. This report will present the design specifications with a high-level solution, a detailed design of the system showing the logic of the micro-controller, a performance evaluation of all stages of the system and a critical analysis.

2. Design specification and high-level solution

Table 1: Showing the design specifications and explanation.

Specifications	**Value**	**Explanation**
Spectral light range (nm)	380-700	To detect the visible light spectrum [1].
Solar Irradiance (W/m^2)	0 – 1350	The photodiode's input range encompassing the modelled signal
Operating Temperature (ºC)	-40 to 100	The photodiode operates over a wide temperature range.
Bandwidth (mHz)	5	Designed to accommodate potential attenuation in signal conditioning
Accuracy	95%	Providing a reliable and effective measurement system
Response Time (seconds)	100	Account for adverse weather patterns.

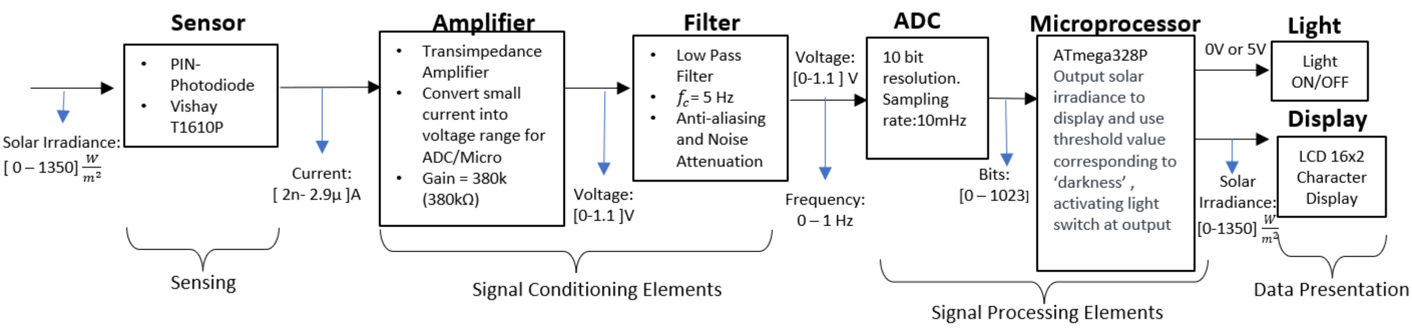

Figure 1: High level solution of the measurement system

3. Detailed design of the remainder of the system.

To model the properties of the pin-photodiode an equivalent circuit was modelled, using the appropriate values to represent its electrical behaviour [2]. The current source (I_{PH}) models the photocurrent which is linearly proportional to the light intensity

[3]. The diode represents the p-n junction of the photodiode [4]. The junction capacitance (C_J) represents the p-n junction's capacitance [4]. The shunt resistance (R_{SH}) denotes the leakage current that bypasses the photodiode [4].

3.1. Amplifier

In order to convert the small current output of the photodiode to voltages, a transimpedance amplifier was designed [5]. The transimpedance gain was determined by dividing the required voltage range (as discussed in section 3.3) by the input range, resulting in a feedback resistor value of 380kΩ. Thereafter, the feedback capacitor was calculated which creates stability and ensures the bandwidth is met [5]. It was calculated using the equation:

$$C_{f1} = \frac{1}{2\,\pi \times R_{f1} \times f_p} \tag{1}$$

Where R_{f1} is the feedback resistor and f_p is the required bandwidth. Therefore, using the feedback resistance and bandwidth established of 5mHz, a feedback capacitor of 85µF was derived [5]. Subsequently, the choice of the operational amplifier was decided by searching for a low output offset voltage [6] and due to the low frequency nature of the input signal, a lower slew rate was deemed acceptable. Ultimately, these specifications were met by the LT6078 [6]. Furthermore, the LT6078's unity gain bandwidth (GBW) of 320kHz was ensured to be sufficiently large as derived by the following equation:

$$GBW > \frac{C_i + C_{f1}}{2\pi \times R_{f1} \times {C_{f1}}^2} \tag{2}$$

Where C_{f1} is the feedback capacitance and C_i is the summation of the input source capacitance, differential input capacitance of the amplifier and common-mode input capacitance of the inverting input [5].

3.2. Filter

To ensure accuracy and reliability of the photodiode measurements, ambient light noise sources such as power line frequencies ,typically oscillating at 50/60 Hz [7] , and flicker noise, typically spanning from tens of Hz to tens of kHz [8] , from other electronic devices or streetlights need to be attenuated [8]. Additionally, attenuating the higher frequency noise reduces the likelihood of aliasing during the analogue-to-digital conversion (ADC).

Therefore, a second-order Butterworth Sallen-Key low-pass filter has been designed with a cut-off frequency of 5Hz with unity gain, resulting in a roll-off rate of -40dB per decade, providing a sufficient roll-off rate to attenuate the ambient light noises and preserving the desired lower-frequency components. To calculate the values of R_1 and R_2 of the filter, $R_1 = m$ and $R_2 = R_n m$ was utilised , where m , the scaling factor was equated to 100kΩ and $R_n = 1$ [9]. Thereafter the following equations were used to calculate C_1 and C_{f2}:

$$C_1 = \frac{0.707}{m \times 2\pi \times f_c} \tag{3}$$

$$C_{f2} = \frac{1.414}{m \times 2\pi \times f_c} \tag{4}$$

The LT6004 operational amplifier, chosen for its low input bias and offset voltage [10], used with unity gain isolates the low pass filter from the ATmega328p thus reducing the loading effects [11]. This ensures a stable and accurate voltage signal is provided to the input of the ADC [11].

3.3. Microcontroller

The ATmega328p's internal voltage reference, ranging from 0V – 1.1V, was chosen as its factory calibration provides more stability and accuracy than an external reference [12], and it eliminates the need for additional components in the circuit. Likewise, a small capacitor was connected between the A_{REF} pin and ground for increased noise immunity [12]. The ADC on the ATmega328P specifies a conversion time of 13-260µs [12], which is more than sufficient to capture a sampling frequency of 10mHz without risking aliasing. Furthermore, the internal ADC's resolution of 10 bits (2^{10} discrete values) is sufficient to cover the range of solar irradiance values, providing a resolution of 1.07mV [11]. The logic of the system design is illustrated in the flowchart presented below:

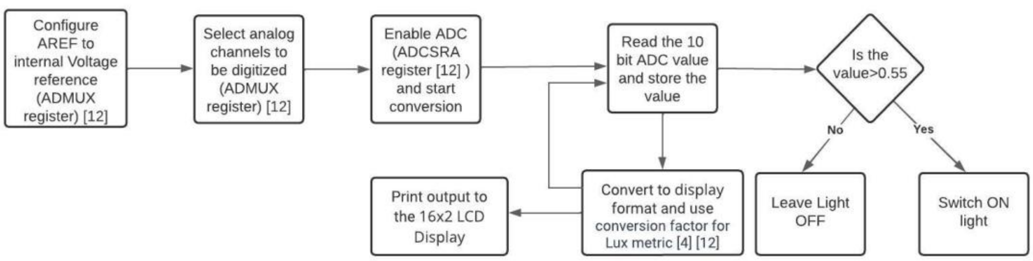

Figure 2: Logic of ADC and Microcontroller

3.4 Display

An LCD 16x2 character display has been chosen for its lower power supply, legibility, durability, and cost effectiveness [13].

4. Performance evaluation

4.1. Transfer Function and Bode plot of system.

The system's total transfer function was derived from cascading all constituent elements and utilising MATLAB for simulation of the dynamic response, the resulting bode plot is shown.

$$H(s) = \frac{3.753 \times 10^8}{31.92s^3 + 2838s^2 + 3.161 \times 10^4 s + 987.6} \qquad (6)$$

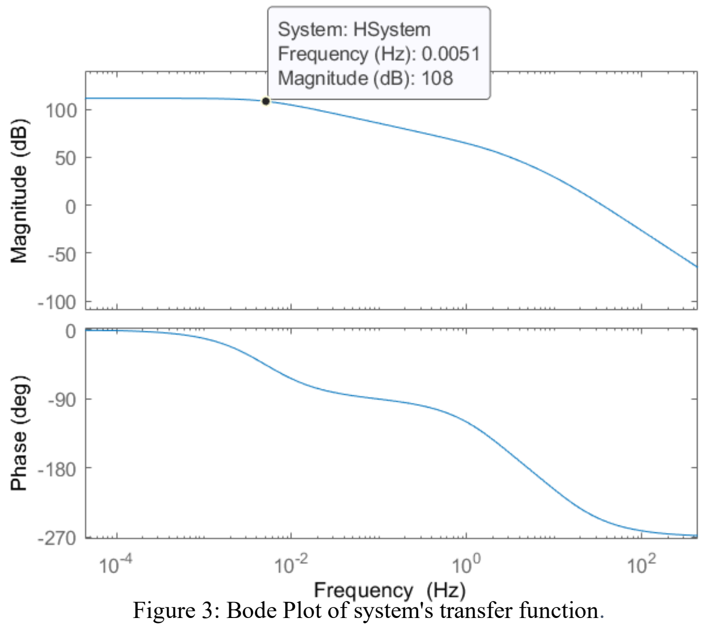

Figure 3: Bode Plot of system's transfer function.

4.2. Table of expected performance specifications

Table 2: Static specifications of light measurement system

Parameter	Value
Spectral Input Range [2]	390nm – 800nm
Photocurrent range [2]	2nA – 2.9 μA
Photosensitivity [2] [11]	$0.0177 \frac{\mathrm{nA}}{\mathrm{Lux}}$
Input ADC resolution [12]	1.07mV
Accuracy	95%

4.3. Error analysis

The pin-photodiode contains two sources of noise: the shot noise and Johnson noise [4]. The shot noise, the statistical fluctuation in the photocurrent range, was calculated to be 1.1046nA [4] [11]. The Johnson noise, due to random thermal motion of the carriers, has a calculated value of 0.0199nA [4] [11]. Therefore, by taking the root square sum of the shot noise and

the Johnson noise, a total sensor error value of 1.1nA which corresponds to a 0.03% error in the photocurrent range was deduced [11]. The 100kΩ resistors have a 1% tolerance [14]and the 380kΩ (a series 3kΩ, 47kΩ and 330kΩ) have a 2.05% tolerance [15] [16][17].
The LT6078 operational amplifier has an input offset voltage of 25μV, which amplified corresponds to a 0.86% error [6]. Likewise, the input offset of the LT6004 is 500 μV, which results in a 0.045% error [10]. The ATmega328p's internal ADC's 10-bit resolution results in a quantisation error of the system is 0.535 mV equivalent of a 0.0486% error [12].

Table 3: Showing errors for all stages and for the overall system.

Stages	Error (%)
Sensing	0.03
Signal Conditioning	4.955
Signal Processing	0.0486
Total (Root sum Square)	4.96

5. Critical analysis

The cost of the measurement system amounts to R336.22 [13] [14] [15] [16] [17] [18]. This amounts to a comparatively expensive solution, despite the increased accuracy. Furthermore, a breakdown of the photodiode would render the measurement system inoperable, therefore, a future improvement could include multiple photodiodes, enhancing maintainability.

The bandwidth of the system was intentionally designed to be to larger than where 99% of the bandwidth was estimated - at 1.288mHz from the power spectral density [19] . Therefore, the cut-off frequency attained in the bode plot of the system of 5mHz (the -3dB point) matches the desired frequency designed in equation (1). The light measurement system aims to improve the safety of children playing on the jungle gym by increasing visibility and allowing parents to view when light levels are low, therefore, providing a safer social environment. Regarding ethics, an environmentally friendly solar panel was chosen for a carbon-free power supply. Additionally, the selection of sensors and components prioritized RoHS compliance and Pb-free materials.

6. Summary and conclusions

In conclusion, the desired measurement system specifications were effectively designed, simulated, and implemented. The required spectral input range, bandwidth of 5mHz and accuracy of 95% were achieved, ultimately providing a realistic and sustainable solution.

References

[1] National Aeronautics and Space Administration, Science Mission Directorate., "Tour of the Electromagnetic Spectrum," NASA Science website:, 2010. [Online]. Available: https://science.nasa.gov/ems/09_visiblelight. [Accessed 20 April 2023].

[2] Vishay Semiconductors, *T1610P Silicon PIN Photodiode,* Document Number: 91000 ed., 2017.

[3] W. Ahmad, U. . A. Muhammad , V. Laxmi and A. . S. Syed, "Simulation and Characterization of PIN Photodiode for Photonic," Asian Journal of Nanoscience and Materials, Islamabad, 2018.

[4] Osi Optoelectronics, *Photodiode Characteristics and Applications,* Hawthorne, CA: Osi Optoelectronics, 2020.

[5] Texas Instruments, *Transimpedance amplifier circuit,* Dallas: Analog Engineer's Circuit: Amplifiers, 2019.

[6] L. Technology, *LTC6078/LTC6079,* LT 0506 REV A ï ed., Milpitasa: Linear Technology Corporation, 2005.

[7] S. Akwei-Sekyere, "Powerline noise elimination in biomedical signals via blind source separation and wavelet analysis," PubMed, Rockville Pike Bethesda, 2015.

[8] . R. F. Voss and J. Clarke, "Flicker (1f) noise: Equilibrium temperature and resistance fluctuations," Physical Review B (Solid State), 1976.

[9] J. Karki, "Analysis of the Sallen-Key Architecture," TEXAS INSTRUMENTS, Dallas, 2002.

[10] Linear Technology, "LT6003/LT6004/LT6005," Linear Technology Corporation, Milpitas, 2005.

[11] J. P. Bentley, Principles of Measurement Systems, Fourth ed., Edinburgh, Essex: Pearson, 2005, pp. 77-95.

[12] "ATmega48A/PA/88A/PA/168A/PA/328/P," Microchip Technology Inc, Chandler, 2020.

[13] Micro Robotics, "LCD 16x2 Character Display, White on Blue Background, 5V," Micro Robotics, 2023. [Online]. Available: https://www.robotics.org.za/LCD-1602-5V-WB. [Accessed 7 May 2023].

[14] Digikey, "MFR-12FTF52-100K," Digi-Key-Electronics, 2023. [Online]. Available: https://www.digikey.co.za/en/products/detail/yageo/MFR-12FTF52-100K/9133807. [Accessed 8 May 2023].

[15] RS , "Panasonic 47000Ω Metal Film SMD Resistor ±0.05% 0.1W - ERA3ARW473V," RS Components, 2023. [Online]. Available: https://za.rs-online.com/web/p/surface-mount-resistors/1809786. [Accessed 8 May 2023].

[16] RS, "RS PRO 330kΩ, 0805 (2012M) Thick Film SMD Resistor ±1% 0.125W," RS - Components, 2023. [Online]. Available: https://za.rs-online.com/web/p/surface-mount-resistors/8046650. [Accessed 8 May 2023].

[17] RS, "RS PRO 3.01kΩ, 0603 (1608M) Thick Film SMD Resistor ±1% 0.1W," RS Components, 2023. [Online]. Available: https://za.rs-online.com/web/p/surface-mount-resistors/7170819. [Accessed 8 May 2023].

[18] Digikey, "Product Index," Digi-Key Electronics, 2023. [Online]. Available: https://www.digikey.co.za/en/products. [Accessed 8 May 2023].

[19] Mathworks, "obw," Mathworks, 2023. [Online]. Available: https://www.mathworks.com/help/signal/ref/obw.html.

Appendix

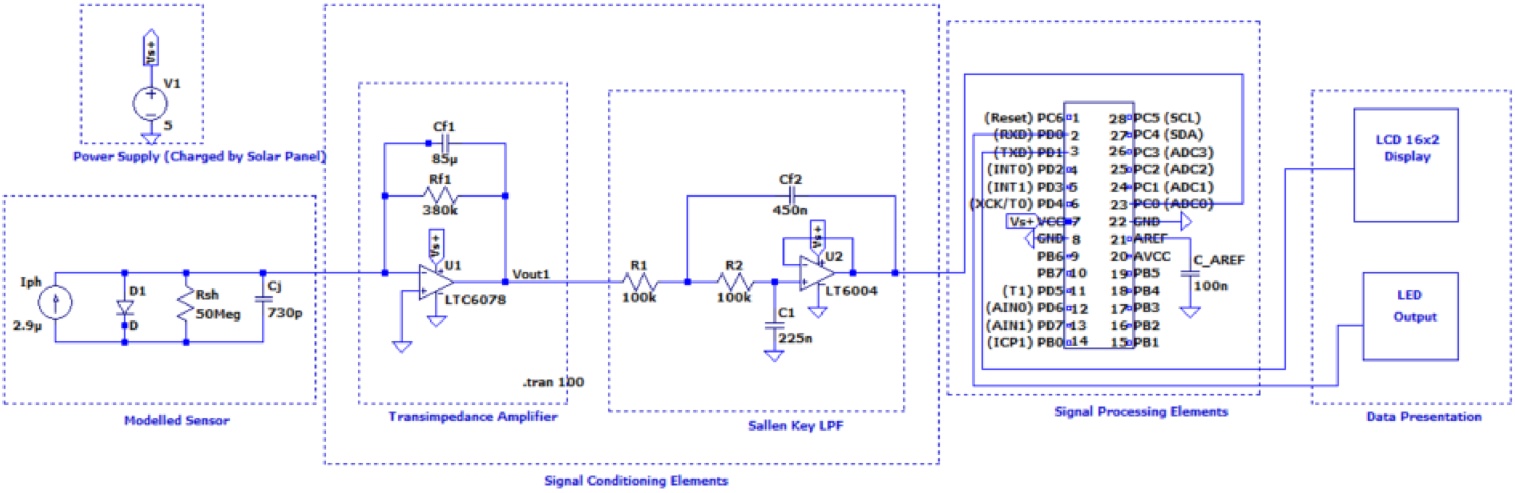

Figure 4: Complete Annotated Circuit Diagram